ISSN 1070-3632, Russian Journal of General Chemistry, 2015, Vol. 85, No. 1, pp. 97–103. © Pleiades Publishing, Ltd., 2015.
Original Russian Text © A.V. Pulya, I.I. Seifullina, L.S. Skorokhod, V.G. Vlasenko, S.I. Levchenkov, V.I. Pavlovskii, 2015, published in Zhurnal Obshchei Khimii, 2015, Vol. 85, No. 1, pp. 105–111.

Characterization of the Coordination Compounds of Co(II) and Ni(II) with 2-(7-Bromo-2-oxo-5-phenyl-3*H*-1,4-benzodiazepin-1-yl)acetohydrazide and Its Condensation Product with Pyruvic Acid

A. V. Pulya[a], I. I. Seifullina[a], L. S. Skorokhod[a], V. G. Vlasenko[b], S. I. Levchenkov[c], and V. I. Pavlovskii[d]

[a] *Mechnikov National University, ul. Dvoryanskaya 2, Odessa, 65082 Ukraine*
e-mail: lborn@ukr.net

[b] *Research Institute of Physics, Southern Federal University, Rostov-on-Don, Russia*

[c] *Southern Research Center, Russian Academy of Sciences, Rostov-on-Don, Russia*

[d] *Bogatskii Physicochemical Institute, National Academy of Sciences of Ukraine, Odessa, Ukraine*

Received September 18, 2014

Abstract—Complexes of Co(II) and Ni(II) with 2-(7-bromo-2-oxo-5-phenyl-3*H*-1,4-benzodiazepin-1-yl)acetohydrazide and its condensation product with pyruvic acid were synthesized and studied. The complexes were characterized by elemental analysis, thermogravimetry, IR and EXAFS spectroscopy, as well as electrical conductivity and magnetic susceptibility measurements.

Keywords: coordination compounds, cobalt(II), nickel(II), 2-(7-bromo-2-oxo-5-phenyl-3*H*-1,4-benzodiazepin-1-yl)acetohydrazide, pyruvic acid, X-ray absorption spectroscopy

DOI: 10.1134/S107036321501017X

Over the past years there has been growing interest in chemical modification of medical substances, including their complexation with biometals. The resulting complexes have a higher activity and a broader spectrum of action [1]. In [2, 3] we described complexes of 3*d* transition metals with organic compounds (piruvic nicotinoyl hydrazides) as potential medicinals. Of particular interest is 2-(7-bromo-2-oxo-5-phenyl-3*H*-1,4-benzodiazepin-1-yl)acetohydrazide (hydazepam), a selective anxiolytic used in medical practice as a daytime tranquilizer [4]. This compound contains a hydrazide moiety, due to which it can be considered not only as an independent ligand, but also as a starting material for the synthesis of hydrazones, in particular, by condensation of pyruvic acid. The vital metal ions Co^{2+} and Ni^{2+} were used as complex-forming agents.

We synthesized Co(II) and Ni(II) complexes with 2-(7-bromo-2-oxo-5-phenyl-3*H*-1,4-benzodiazepin-1-yl)acetohydrazide (Hydr) and its condensation product with pyruvic acid (HPv) and studied their structure and properties. As seen from the elemental analyses (Table 1), the reactions of the hydrazide with $CoCl_2$ and $NiCl_2$ form complexes **I** and **II** with $CoCl_2$–Hydr and $NiCl_2$–Hydr molar ratios of 1 : 1 (**I**) and 1 : 2 (**II**), respectively. Attempted direct condensation of the hydrazide with pyruvic acid failed. Isolable complexes $[Co(HydrHPv)Cl_2]\cdot 2H_2O$ (**III**) and $[Ni(HydrPv)_2]$ (**IV**) (HydrHPv is the condensation product of Hydr and HPv) could only be obtained in MCl_2–Hydr–HPv ternary systems (Tables 1 and 2).

Compounds **I**–**IV** are fine crystals insoluble in methanol, ethanol, propan-2-ol, chloroform, and acetonitrile and soluble in DMSO, DMF, and a hot nitrobenzene. The electrical conductivities of 1×10^{-3} M solutions of complexes **I**–**IV** in DMSO (Table 1) show that the complexes are nonelectrolytes.

Thermolysis of complexes **I**–**III** occurs in steps. The first, low-temperature endothermic effect in compounds **I** and **III** is associated with elimination of

Table 1. Characteristics of complexes **I–IV**

Complex	Color	Λ_m, Ω^{-1} cm^2 mol^{-1}	μ_{eff}, BM (293 K)
$[Co(Hydr)Cl_2]\cdot H_2O$ (**I**)	Blue	13.6	4.37
$[Ni(Hydr)_2Cl_2]$ (**II**)	Light green	32.0	3.30
$[Co(HydrHPv)Cl_2]\cdot 2H_2O$ (**III**)	Bright blue	13.0	4.20
$[Ni(HydrPv)_2]$ (**IV**)	Grayish blue	24.8	3.26

Table 2. Elemental analyses of complexes **I–IV**

Complex	Found, %						Formula	Calculated, %					
	C	H	Br	Cl	N	M^{2+}		C	H	Br	Cl	N	M^{2+}
$[Co(Hydr)Cl_2]\cdot H_2O$ (**I**)	37.84	3.09	14.84	13.15	10.16	10.91	$C_{17}H_{17}BrCl_2N_4O_3Co$	38.13	3.18	14.95	13.27	10.47	11.03
$[Ni(Hydr)_2Cl_2]$ (**II**)	44.90	3.21	17.56	7.69	12.08	6.31	$C_{34}H_{30}Br_2Cl_2N_8O_4Ni$	45.13	3.32	17.70	7.85	12.39	6.53
$[Co(HydrHPv)Cl_2]\cdot 2H_2O$ (**III**)	38.19	3.19	12.66	11.29	8.71	9.19	$C_{20}H_{21}BrCl_2N_4O_6Co$	38.52	3.37	12.84	11.40	8.99	9.47
$[Ni(HydrPv)_2]$ (**IV**)	49.28	3.18	16.64	–	11.62	5.96	$C_{40}H_{32}Br_2N_8O_8Ni$	49.43	3.30	16.48	–	11.53	6.08

water of crystallization. Further thermolysis of complexes **I–III** involves elimination of two HCl molecules, which is accompanied by the following endothermic effect: second for **I**, first for **II**, and second and third for **III**. Further heating of compounds **I–III** leads to deep thermo-oxidative degradation of the organic part of the molecules, as evidenced by a series of high-temperature exothermic effects. Unlike what is observed with complexes **I–III**, the TG curve of complex **IV** contains no low-temperature endothermic effects, and this is consistent with the results of elemental analysis (absence of chloride ions and water molecules). Complex **IV** melts with decomposition at 360°C. The final thermolysis products of complexes **I**, **III** and **II**, **IV** are Co(II) and Ni(II) oxides, respectively, which agrees with the weight losses in the TG curves.

The coordination mode of ligands in complexes **I–IV** was determined using IR spectroscopy by comparing characteristic absorption bands of the starting ligands and corresponding complexes. In the IR spectra of complexes **I** and **II**, the ν(NH) and ν(NH_2) bands [3267, 3392 cm^{-1} (**I**); 3261, 3408 cm^{-1} (**II**)] are shifted red compared to the hydrazide (3337, 3429 cm^{-1}) due to binding of the latter to M^{2+}. The IR spectra of complexes **I** and **II** also show shifting and changing of the shape of the ν(C=O) bands: 1655 sh, 1678 (Hydr); 1664 (**I**), 1663 (**II**) cm^{-1}. Two new bands appear: ν(M–O) [545 (**I**), 545 cm^{-1} (**II**)] and ν(M–N) [420 (**I**), 458 cm^{-1} (**II**)].

Comparing the IR spectra of the ligands and complexes **III** and **IV** we note the absence of the ν(NH_2) bands and appearance of a new band ν(C=N) at 1539 (**III**) and 1540 cm^{-1} (**IV**). Consequently, the ligand in complexes **III** and **IV** is hydrazone. The pyruvic carboxyl in complex **III** is not involved in coordination, as evidenced by the fact that its IR spectrum contains the carboxyl ν(C=O) band at 1681 cm^{-1}. The band at 1669 cm^{-1} most likely belongs of the ν(C=O) band of the hydrazide fragment. The IR spectrum of complex **IV** contains no band of a carboxy group, which can be interpreted in terms of deprotonation and monodentate binding to Ni^{2+} [$\Delta = \nu_{as}(CO_2^-) - \nu_s(CO_2^-) =$ 246 cm^{-1}] [5]. This interpretation is consistent with the appearance of new bands: ν(M–O) at 543 (**III**), 544 cm^{-1} (**IV**) and ν(M–N) at 418 (**III**), 456 cm^{-1} (**IV**).

Further information on the structure of the coordination entity in complexes **I, III,** and **IV** was obtained by means of EXAFS spectroscopy. One of the characteristic features of the XANES spectra of metal complexes is the presence (or absence) of weak pre-edge peaks. The position of the pre-edge peaks on the energy scale, as well as their fine structure and intensity depend on the geometry of the coordination

entity and the chemical composition of the nearest coordination spheres. Normalized Co(Ni) *K*-edge XANES spectra of complexes **I, III,** and **IV** are presented in Figs. 1 and 2, respectively. The inserts in the figures show the near-edge spectra and their first derivatives.

As seen from Fig. 1, the XANES shapes and energy characteristics for complexes **I** and **III** are similar to each other, implying similar geometries of the local environment of the Co^{2+} ion in these complexes. The Co *K*-edge spectra of complexes **I** and **III** contain strong pre-edge peaks A associated with $1s \rightarrow 3d$ electron transitions [6] which are dipole-forbidden for 3*d*-metal *K* edges. This forbiddance is cancelled by $4p$–$3d$ hybridization of metal AOs, which takes place exclusively in low-symmetry complexes (hybridization is strictly forbidden for centrosymmetric coordination polyhedra, for example, octahedra; in these cases, the intensity of the pre-edge peak is primarily associated with $1s \rightarrow 3d$ quadruple transitions which contribute two orders of magnitude less than dipole). The high amplitude of peaks *A* in the XANES spectra of

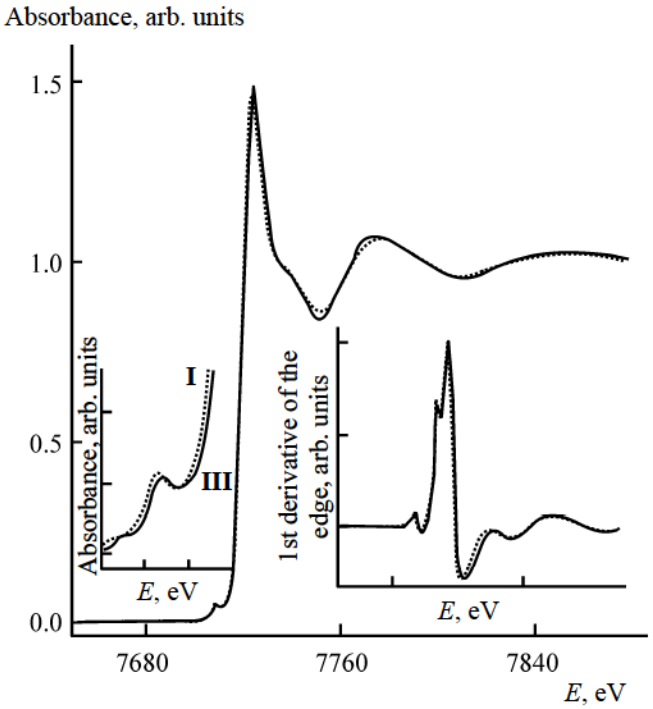

Fig. 1. Cobalt *K*-edge XANES spectra and their first derivatives for complexes (dashed line) **I** and (solid line) **II**.

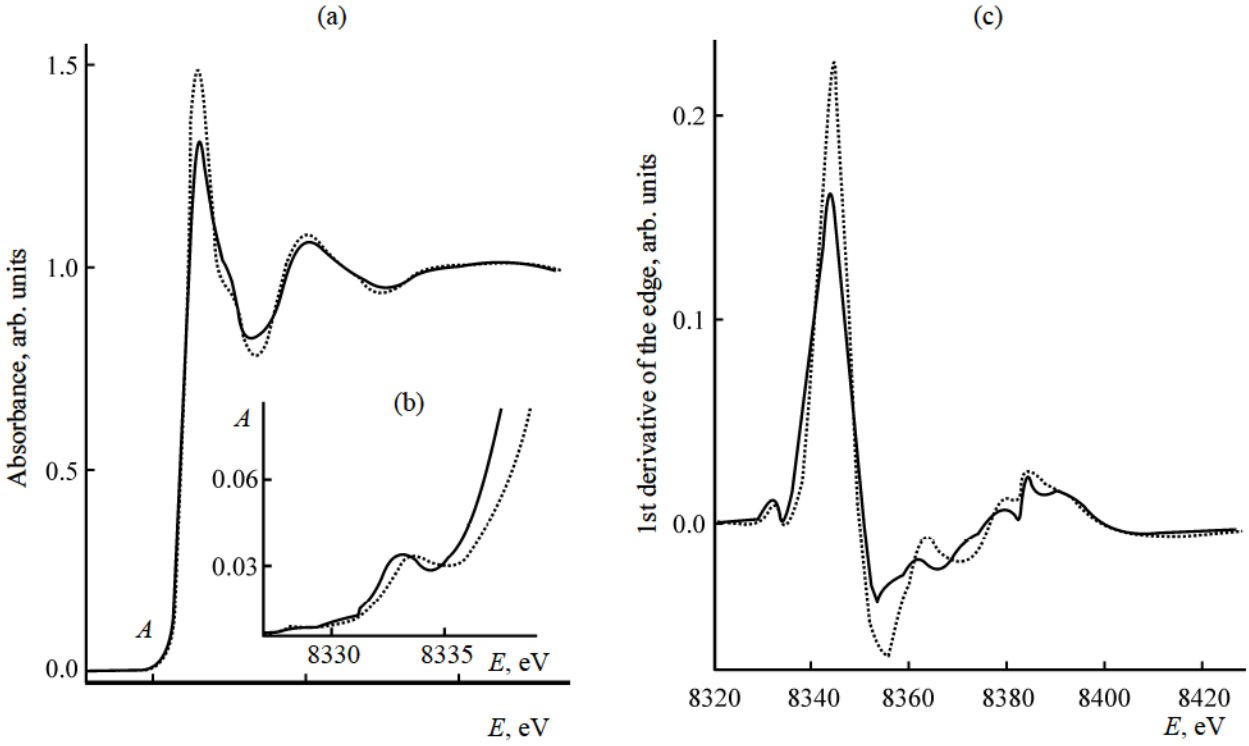

Fig. 2. (a) Nickel *K*-edge XANES spectra of complexes (dashed line) **I** and (solid line) **II**, (b) pre-edge region, and (c) corresponding first derivatives of the edges.

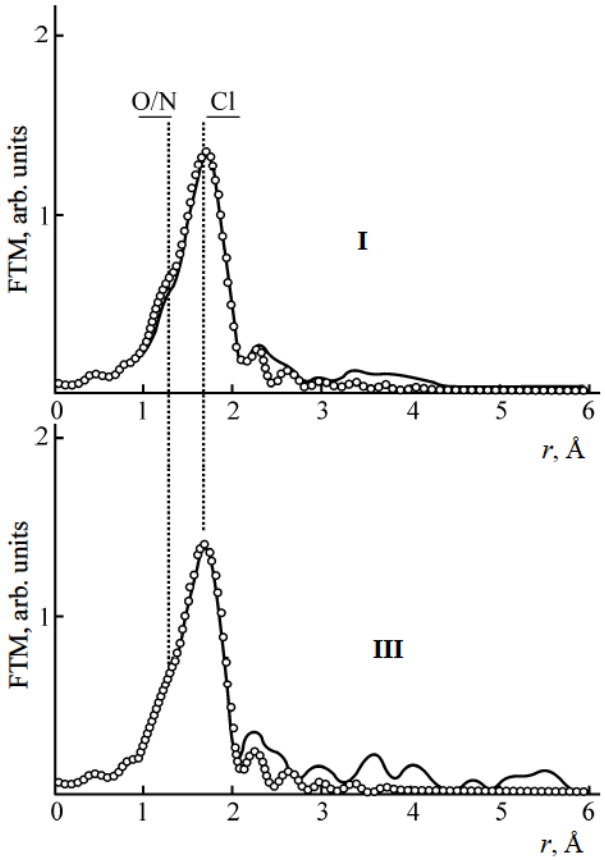

Fig. 3. Fourier-transformed Co *K*-edge EXAFS spectra of cobalt complexes **I** and **III**.

complexes **I** and **III** points to a low-symmetry environment of the cobalt ions, for example, tetrahedral, which has no inversion center and allows 4*p*–3*d* hybridization of cobalt AOs.

The XANES fine structure directly at the edge and in the post-edge region up to ~50 eV is primarily associated with the $1s \rightarrow 4s$ and $1s \rightarrow 4p$ transitions coupled with ligand-to-metal shakedown transitions (Fig. 1, edge features *B* and *C*). The first derivative of the edge in the spectra of complexes **I** and **III** has two main maxima, which suggests a possible tetrahedral environment of the cobalt atom in these compounds.

The XANES spectrum of nickel complex **IV** (Fig. 2) has lines *B* characteristic of complexes with the absorbing ion surrounded by light atoms. The A peak in the Ni *K*-edge absorption pre-edge structure, associated with the 4*p*–3*d* mixing is not very strong but appreciable, implying that the geometry of the environment is different from octahedral. At the same time, the first derivative of the Ni *K*-edge absorption of **IV** looks like a series of strong narrow peaks characteristic of an octahedral environment. The above evidence together suggests a distorted octahedral geometry of the coordination entity in complex **IV**.

Quantitative characteristics of the local atomic environment cobalt complexes **I** and **III** and nickel complex **IV** were obtained from an analysis of the Co and Ni *K*-edge X-ray absorption spectra.

The Fourier transform modules (FTM) of the Co *K*-edge EXAFS signals of complexes **I** and **III** (Fig. 3) are similar to each other and contain a peak at low *r* value (a shoulder in the FTM), which is uniquely associated with scattering in the local coordination sphere comprising the nitrogen and oxygen atoms of the ligands, as well as a large-amplitude peak (*r* 2.70 Å), which, in view of the ligand structure, can be assigned to scattering in the second coordination sphere comprising chlorine atoms. The best fitting results were obtained with two O/N couples at distances of 2.02 Å and two chlorine atoms in the second coordination sphere with a radius of 2.24 Å, which provides evidence for a tetrahedral structure of complexes **I** and **III**.

Table 3 lists the composition and characteristics of the nearest coordination spheres (coordination numbers, radii, and Debye–Waller factors), obtained by fitting calculated to experimental EXAFS data for complexes **I** and **III**.

With Ni^{2+} complex **IV**, along with traditional analysis of EXAFS using Fourier transform, to estimate the $\chi(k)$ function we used wavelet transform (WT) [7], which allows one to differentiate scattering from different atoms in the same coordination sphere.

Figure 4 shows the Fourier-transformed EXAFS spectra of complex **IV** and two-dimensional WT maps of the wavelet-transformed EXAFS function in the *r*–*k* coordinates. The FTM has the main peak at *r* 1.6–1.65 Å, associated with the first coordination sphere comprising light atoms. At larger distances lower-amplitude peaks are also observed. The wavelet analysis shows that these peaks, too, belong to coordination spheres comprising light atoms, which rules out the model of dimer formation and is consistent with the temperature dependence of magnetic susceptibility.

The quantitative characteristics of the coordination sphere for the resulting model (Table 3) show that the local environment of the nickel ion in complex **IV** consists of 6 nitrogen and oxygen atoms at different

Table 3. Structural characteristics of the nearest environment of the metal atom in cobalt complexes **I** and **III** and nickel complex **IV**, obtained by fitting EXAFS spectral data

Complex	N	R, Å	σ^2, Å^2	Atom	Q, %
I	2	2.02	0.0040	O/N	0.9
	2	2.24	0.0045	Cl	
III	2	2.02	0.0030	O/N	1.6
	2	2.24	0.0045	Cl	
IV	3	2.01	0.0035	O/N	0.5
	3	2.16	0.0035	O/N	

distances. Thus we obtained evidence for an octahedral geometry of the coordination entity.

The above findings and magnetic susceptibility measurements (Table 1) allowed the complexes to be assigned structures **I**–**IV** (Scheme 1).

EXPERIMENTAL

The IR spectra (4000–400 cm^{-1}) were recorded on Perkin–Elmer Spectrum BX-IIFI-IR and Shimadzu FTIR-8400S spectrophotometers in KBr. Thermogravimetry was performed on a Paulik–Paulik–Erday Q-derivatograph. Samples were heated in air from 20 to 1000°C at a rate of 10 deg/min. A 60–80-mg sample was put in an uncovered platinum crucible, the reference was calcined alumina.

The molar electrical conductivities of 1×10^{-3} M solutions of complexes **I**–**IV** in DMSO were measured by an Economics Expert digital meter, the type of electrolyte was determined according to [8]. Magnetochemical measurements were performed on a Quantum Design MPMS XL-5 SQUID magnetometer in the temperature range 5–300 K, magnetic field 5 kOe. The molar magnetic susceptibilities (χ_m) were calculated taking into account the atomic diamagnetism by the Pascal additive scheme [9]. The effective magnetic moments were calculated by Eq. (1).

$$\mu_{eff} = \sqrt{(3k/N\mu_B)\chi T} \approx \sqrt{8\chi T}. \quad (1)$$

Here k is the Boltzmann constant; N, Avogadro number; and μ_B, Bohr magneton.

The K-edge X-ray absorption spectra of cobalt (**I, III**) and nickel (**II, IV**) were obtained on an EXAFS spectrometer at the Structural Materials Science end-station, Kurchatov Center for Synchrotron Radiation and Nanotechnology. The electron beam energy was 2.5 GeV at a current of 80–100 mA. Monochromatic X-ray radiation was generated using a double-crystal Si(111) monochromator. Solid samples were placed between thin lavsan films. The spectra were processed by standard procedures including background subtraction, K-edge step normalization, and correction for atomic absorption μ_0 [10], after which Fourier transformation of the EXAFS (χ) spectra in the photoelectron wave vector (k) range from 3.0 to 13.0 Å^{-1} with the weight function k^3. The resulting Fourier transform modules are pseudoradial distributions of atoms in the nearest coordination spheres of absorbing atoms (cobalt or nickel), with radii calculated to an accuracy of phase corrections. The threshold ionization energy E_0 was chosen as the maximum of the first derivative of the K-edge spectrum and then varied on fitting.

To interpret the results of EXAFS measurements, the experimental absorption spectrum $\chi(k)$ was fitted by function (2).

$$\chi(k) = S_0^2 \sum_{i=1}^{n} \frac{N_i}{R_i^2} \frac{F_i(k)}{k} e^{-2R_i/\lambda} e^{-2\sigma_i^2 k^2} \sin(2kR_i + \Psi). \quad (2)$$

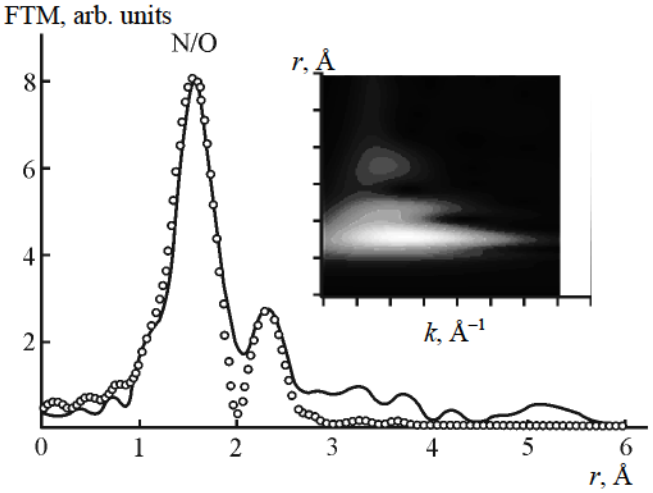

Fig. 4. (a) Fourier-transformed Ni K-edge EXAFS spectrum of complex **IV** and (b) WT map in the r–k coordinates of the wavelet-transformed EXAFS spectrum.

Scheme 1.

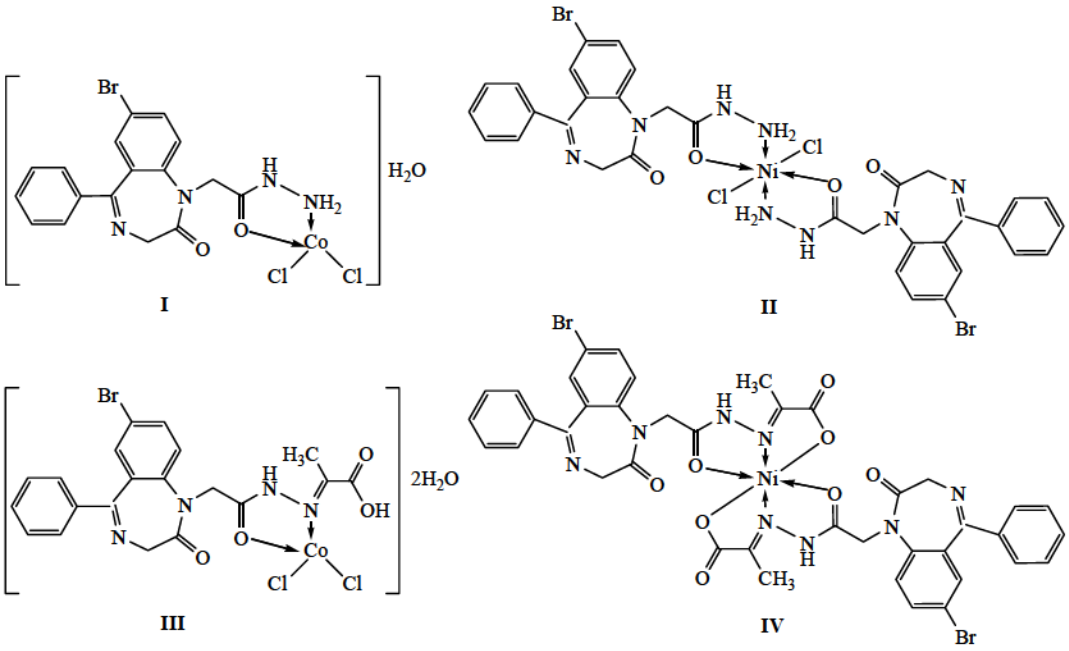

Here N_i is the number of atoms in the ith coordination sphere; R_i, average radius of the coordination sphere; σ_i^2, Debye–Waller factors; $F_i(k)$, back scattering amplitude; and k, ejected electron wavelength.

The exact structural parameters of the local environment of the cobalt and nickel atoms in complexes **I**–**IV** were determined by nonlinear fitting of the calculated EXAFS signal to that isolated from the full EXAFS spectrum by Fourier transformation using IFFEFIT-1.2.11 suite of programs [11]. The photoelectron wave phases and scattering amplitudes were calculated using FEFF7 program [12], with atomic coordinates for compounds with a similar atomic structure.

The number of parameters varied in multisphere fitting was never larger than the number of the independent parameters N_{ind} which can be reliably calculated by Eq. (3) from the EXAFS spectra in the present Δk and Δr ranges.

$$N_{ind} = (2\Delta r \Delta k/\pi) + 1. \quad (3)$$

Here Δk is the analyzed region of the EXAFS spectrum in the space of photoelectron wave vectors and Δr, Fourier-filtered R-space region.

The GOF function Q minimized in the optimization of the structural parameters of the local environment was calculated by Eq. (4).

$$Q(\%) = \frac{\Sigma[k\chi_{exp}(k) - k\chi_{th}(k)]^2}{\Sigma[k\chi_{exp}(k)]^2} \times 100\%. \quad (4)$$

Analysis of compounds **I**–**IV** for carbon, hydrogen, and nitrogen was performed on a CHN analyzer, for total chlorine and bromine, by mercurometry [13], and for cobalt and nickel, by inductively coupled plasma atomic emission spectroscopy on an Optima–2100 DV Perkin Elmer instrument.

Complexes I and **II.** To a solution of 0.002 mol of 2-(7-bromo-2-oxo-5-phenyl-3*H*-1,4-benzodiazepin-1-yl)acetohydrazide (Hydr) in 20 mL of isopropanol, a solution of $CoCl_2 \cdot 6H_2O$ (or $NiCl_2 \cdot 6H_2O$) in 10 mL of ethanol (MCl_2–Hydr molar ratio 1:2) was added with stirring. The reaction mixture was heated under reflux on a water bath for 0.5 h. The precipitate of complex **I** (or **II**), that formed after cooling, was filtered off, washed with isopropanol and ethanol, and dried at 80°C to constant weight.

Complexes III and **IV.** To a solution of 0.002 mol of 2-(7-bromo-2-oxo-5-phenyl-3*H*-1,4-benzodiazepin-1-yl)acetohydrazide (Hydr) in 20 mL of isopropanol, 0.002 mol of pyruvic acid (HPv) and a solution of $CoCl_2 \cdot 6H_2O$ (or $NiCl_2 \cdot 6H_2O$) in 10 mL of ethanol was added (MCl_2–Hydr–HPv molar ratio 1 : 2 : 2). The reaction mixture was heated under reflux for 1 h, cooled, and then treated as described for complexes **I** and **II** to obtain complexes **III** and **IV**.

REFERENCES

1. Basareva, O.I., Zaikin, A.V., Khapchaeva, D.A., Kostrov, S.V., Bukreeva, E.V., Kalutskii, P.V., and Lazurina, L.P., *Kursk. Nauch.-Prakt. Vestn. "Chelovek i ego Zdorov'e,"* 2007, no. 4, p. 5.
2. Pulya, A.V., Seifullina, I.I., Skorokhod, L.S., and Vlasenko, V.G., *Russ. J. Gen. Chem.*, 2013, vol. 83, no. 9, p. 1673. DOI: 10.1134/S1070363213090089.
3. Pulya, A.V., Seyfullina, I.I., and Shmatkova, N.V., *Visn. ONU*, 2011, vol. 16, no. 4, p. 32.
4. Andronati, S.A., Yavorskiy, A.S., Zhilina, Z.I., Yakubovskaya, L.N., Chepelev, V.M., Pyatin, B.M., Shcherbakova, O.V., Arystanova, P.A., Golovenko, N.Ya., Zin'kovskiy, V.G., Zhuk, O.V., Stankevich, E.A., Zherdev, G.B., Kolyvanov, G.B., Lyganov, S.I., Voronina, T.A., Nerobkova, L.N., Bogdanov, N.N., Markina, N.V., Garibova, T.L., Kalinina, T.S., Voronin, K.E., Seredenin, S.B., Blednov, Yu.A., Durnev, A.D., Gordey, M.L., Kozlovskaya, M.M., Rakhmankulova, Yu.A., Belozertsev, Yu.A., Grigor'eva, N.D., Rudenko, L.P., Molodavkin, G.M., Ramkhin, E.Ya., Lyubimov, B.I., Smol'nikova, N.M., Sorokina, A.V., Kovalenko, L.P., Muzychenko, A.P., Neznamov, G.G., Lygalov, S.I., Bochkarev, V.K., Kolyvanov, G.B., Zharikov, N.M., Morozov, I.S., Barchukov, V.G., Zhirnov, E.N., Ivanets, N.N., Kipervas, I.P., Starodubtsev, A.K., Khairetdinova, N.B., Goncharov, K.O., Skibitskii, V.V., Bitenskii, V.S., Savostin, A.P., and Andronati, I.S., *Gidazepam* (Hydazepam), Kiev: Naukova Dumka, 1992.
5. Nakamoto, K., *Infrared and Raman Spectra of Inorganic and Coordination Compounds*, New York: Wiley, 1963.
6. Yamamoto, T., X-Ray Spectrom., 2008, vol. 37, p. 572. DOI: 10.1002/xrs.1103.
7. Funke, H., Chukalina, M., and Scheinost, A., *J. Synchrotron Rad.*, 2007, vol. 14, p. 426. DOI:10.1107/S0909049507031901.
8. Geary, W.J., *Coord. Chem. Rev.,* 1971, vol. 7, p. 81. DOI: 10.1016/S0010-8545(00)80009-0.
9. Rakitin, Yu.V. and Kalinnikov, V.T., *Sovremennaya magnetokhimiya* (Modern Magnetochemistry), St. Petersburg: Nauka, 1994.
10. Kochubei, D.I., Baranov, Yu.A., Zamaraev, K.I., Vedrinskii, R.V., Kraizman, V.L., Kulipanov, G.N., Mazalov, L.N., Skrinskii, A.N., Fedorov, V.I., Khel'mer, B.Yu., and Shuvaev, A.T., *Rentgenospektral'nyi metod izucheniya struktury amorfnykh tel: EXAFS-spektroskopiya* (X-ray Spectral Method of Study of the Structure of Amorphous Substances: EXAFS Spectroscopy), Novosibirsk: Nauka, Sib. Otd., 1988.
11. Newville, M., *J. Synchrotron Rad.*, 2001, vol. 8, p. 96. DOI: 10.1107/S0909049500016290.
12. Zabinski, S.I., Rehr, J.J., Ankudinov, A., and Alber, R.C., *Phys. Rev.*, 1995, vol. 52, p. 2995. DOI: http:,dx.doi.org/10.1103/PhysRevB.52.2995.
13. Klyuchnikov, N.G., *Rukovodstvo po neorganicheskomu sintezu* (Manual on Inorganic Synthesis), Moscow: Khimiya, 1965, p. 104.